

Recovery of Strategic Metals from Tungsten Carbide-Cobalt Bonded Waste by Electrochemical Processing

Prvan Kumar Katiyar¹ and Navneet Singh Randhawa^{2*}

¹*Department of Metallurgical and Materials Science Engineering,
National Institute of Technology, Srinagar, 190006, India*

²*Metal Extraction and Recycling Division, CSIR-National Metallurgical Laboratory,
Jamshedpur-831007, India*

*Corresponding author: nsrandhawa@gmail.com, nsr@nmlindia.org

Received 29/09/2021; accepted 10/01/2022

<https://doi.org/10.4152/pea.2023410202>

Abstract

Scraped or end-of-life WC-Co bonded makes it an attractive resource. The conventional technologies to recover these metals entail energy-intensive pre-treatment steps, followed by their dissolution in a high volume of concentrated acids/alkali reagents. Recently, much attention has been given to the development of energy-efficient and environmentally friendly routes based on WC-Co direct electrochemical dissolution as anodes. However, the metals have a retarded dissolution, in NaOH alkali media, due to the formation of passive oxide layers, in the acidic electrolytes, and of hydroxides, on the anodic surface. The present study investigated WC and Co dissolution fundamentals in aqueous NH₃, in order to develop a greener process, by the suitable addition of (NH₄)₂CO₃, (NH₄)₂SO₄ and NH₄Cl Preliminary PDP studies revealed the necessary concentration of NH₃ and additives, and their effect on the metals passivation tendency, for obtaining the best anodic dissolution parameters. The electrodisolution experiments in a specially designed cell achieved the maximum values, by adjusting those parameters. The highest dissolution of W and Co occurred under optimum conditions (10 V, 150 g/L NH₃ and 15% w/v NH₄Cl). Co was deposited at the cathode, while H₈N₂O₄W remained in the electrolyte and was recovered as H₂WO₄ or YTO. Topographical analysis of the polarized surface by AFM has confirmed the pitting corrosion mechanism responsible for W and Co dissolution. A process flow chart for the newly developed single-step direct recycling methods of WC scraps has also been proposed. This process has produced pure saleable WO₃ powder and Co.

Keywords: WC-Co scrap, recycling, NH₃ electrolyte, PDP, electrodisolution, WO₃ and Co.

Introduction*

W and Co are strategic metals, due to their inherent properties and critical applications. W carburization by C generates WC, which, when mixed with Co by

* The abbreviations list is in pages 130-131.

powder metallurgical route, via a liquid phase sintering process, produces cemented WC-Co. This alloy possesses exotic properties, such as very high hardness, excellent wear resistance, superior toughness and outstanding corrosion resistance [1]. Due to these properties, WC-Co finds applications in cutting tools, seal rings, drill bits, and various mining equipment. Table 1 shows general characteristics of W, C and WC-Co.

Table 1. Some characteristics of WC-Co and its constituent metals.

Symbol	W (atomic)	Co (atomic)	WC-Co
Mass (g/Mol.)	183.86	58.93	195.86
Bulk density (g/cm ³)	19.3	8.90 g/cm ³	15.63
Melting point (°C)	3410	1495	2870
Boiling point (°C)	5530	2927	6000
Solubility in water	-	-	Insoluble
Nominal specific gravity	19.25	8.92	14.29
Particle shape	-	-	Irregular
Appearance	-	-	Grey-black lustrous
Crystallography	BCC	HCP	Hexagonal

However, WC-Co materials have often worn out and failed, due to extreme environmental conditions [2] during drilling or tunnel construction, for various industries, such as oil, gas, petroleum and mining exploration [1]. As the global consumption of these materials grows due to an increasing population, the requirement for manufactured goods will also rise. Since W and Co are rare and valuable materials, and their extraction is also energy extensive and costly, many potential sources of WC-Co based scraps could be turned out into valuable secondary resources [3]. These sources include worn-out discarded or failed WC-Co tool bits (from cutting, drilling and mining) and machining scraps. WC scraps also come from wear-resistant parts and high-temperature applications, such as turbine blades, jet nozzles, or other parts removed from jet engines, hard metal residues, tailings, machined chips, grindings and armament industry (various anti-aircraft and anti-missile warheads/ammunition). Hence, various types of W scraps are generated, either during the manufacturing of W alloys materials, or at the end of their service life [1, 4]. The recycling of scrapped WC, W and Co alloys has numerous benefits, due to the following reasons: (i) W and Co concentration in ores is considerably lower (30-99%) than that of their various types of scraps, which results in their high-cost extraction, and in the emission of toxic gases; associated elements in scraps do not cause severe problems during chemical processing; and contaminated metal contents are lower and better known in scraps than in ores. So, WC-Co scrapped materials recycling would be eco-friendly and more economical than extracting these metals from the ore. Hence, scrapped WC-Co materials can be embodied as an excellent secondary resource, with a view of recovering these metals, which can be considered strategically very important, in order to cut the emission of toxic gases and save time [5]. Besides, statistics reveal that approxim. 20 to 30% of the total

supply of recovered W and Co may drop the raw material cost by about 15 to 50% [6].

Although several recycling processes have been globally developed and used, their success would depend on their eco-friendliness and economic feasibility [5]. These processes include pyrometallurgy-based oxidation, carbothermal reduction [7, 8] hydrometallurgy [9, 10] and electrometallurgy [11-18] routes, or their combination [19-21], in order to recover the valuables W and Co materials. Researchers [4] have also studied pyrometallurgy [8], hydrometallurgy [10, 22] or pyro/hydrometallurgy [19]) methods, and compared them based on energy consumption, eco-friendliness, equipment cost, emission of toxic gases and recovery of different products (e.g., W and Co) [23].

The major pyrometallurgical-based recycling processes are Zn melting [24, 25], cold streaming, chemical modification, alkali leaching [26], oxidation roasting followed by leaching [19], chlorination, high-temperature smelting, molten salts electrolysis [27], etc., of which majority involves the use of expensive chemicals (acids, bases, and inorganic salts). A mechano-chemical reaction-based recycling process, in which the scrapes were thermally oxidized at 600 °C, followed by grinding in NaOH, and water leaching, has also been developed [29].

Zn melting allows a direct conversion of the waste containing WC into a usable powder, by Co selective dissolution in a molten Zn bath. Although it (and also cold streaming) does not involve the numerous steps of conversion, extraction, precipitation, etc., from other methods, which increase the recycling time and costs, Zn melting is not economical, since it involves crushing (grinding, milling) scrapes, also demanding much energy. Further refining by chemical modification is essential to attain more pure W, but it requires large-scale equipment, more expensive than the direct recycling practice, and it yields a relatively slow reaction rate [28].

Therefore, the pyrometallurgical-based processes suffer from disadvantages, such as high energy consumption, emission of toxic gases that cause pollution, and stringent air filtration.

On the other hand, hydrometallurgical methods involve the use of corrosive and concentrated acids for dissolving WC-Co material of the refractory type. Besides, they usually require subsequent separation and purification processes, which are also relatively time-consuming.

Electrochemical-based recycling methods have advantages over hydrometallurgical and pyrometallurgical processes, such as lower energy consumption, higher efficiency, lower costs, and less industrial requirements [4]. So, since suitable electrochemical recycling processes, in order to recover pure W and Co from WC-Co scrap materials, are fundamental [30], the interested research community has started their development, by collecting and sorting WC scrapes.

In an electrochemical process, the WC-Co scrapes act as the anode, and graphite or SS are used as the cathode. During electrolysis, the anode and cathode are dipped into the selective electrolyte. A DC power source provides the power supply to the electrochemical cell, in which the positive and negative terminals are connected to the anode (scrap materials) and the cathode, respectively. During electrolysis, the

anodic material dissolution starts, and both Co and W dissolve in a solution containing their ions. Two different types of electrochemical recycling techniques based on HCl, HNO₃, H₂SO₄, H₃PO₄ and alkali electrolytes (NaOH and NH₃) have been adopted in the WC-Co scrap electrodisolution. It has been found that W and Co effective recovery depend on the selective phase dissolution and deposition mechanisms [6, 15, 16, 19, 28, 31-37]. However, in an acidic medium, Co is dissolved and goes into the electrolyte, and a significant fraction of it is deposited on the cathode, leaving behind the WC skeleton as an anode residue, which is further processed. After dissolution, the undissolved WC anode residue materials are obtained from the bottom of the cell and, then, subjected to crushing and drying, in order to obtain, by electroextraction, the W powder. However, the remaining Co is simultaneously deposited on the cathode or removed from the electrolyte, by using the electrowinning process.

The foremost constraints of this technique are that it is time consuming, still suffers from anodic passivation, and its use of aggressive chemicals causes the corrosion of costly equipment. This makes the procedure relatively inefficient and more expensive than the pyrometallurgical-based process. However, the main benefit of this technique is to obtain very pure W and Co, in a single-step direct recycling process [6, 37]. On the other hand, WC scrap electrodisolution in a NaOH electrolyte has constraints, since this electrolyte recycling is impossible, and further conversion of Na₂WO₄ into H₈N₂O₄W is very time-consuming. Alternatively, the WC-Co scraps have also been treated in an alkali medium of NH₄OH (high pH), because W and Co are highly soluble in it, forming H₈N₂O₄W or APT and Co amine complexes [12, 16, 19, 34]. Further processing of the obtained APT, at high temperatures, under H₂ gas, leads to the formation of W powder [38]. However, it has also been reported that the anodic passivation retards the scrap dissolution and adversely affects metals recovery [28].

Considering these facts, a systematic study on cemented WC scrap electrodisolution in NH₃ electrolytes has been carried out, in order to develop an improved process for the recovery of valuable refractory and strategic metals, such as W and Co. PDP tests were conducted for understanding the WC-Co scrap electrochemical anodic dissolution mechanisms and passivation behavior. PDP also indicated the suitable electrolyte composition and the best additives, so as to ensure the WC-Co samples uninterrupted dissolution. AFM micrographs have confirmed the dissolution mechanisms, and their extent, based on the R_a value. The YTO and Co metals were obtained by the subsequent electrolyte processing.

Experimental procedures

Testing material and chemicals

Cemented WC-Co tool bits scraps

Cemented WC-Co tool bits were supplied by M/s Bharat Futuristic Pvt. Ltd, Bangalore, India. Most of the scraps had some brazing material left over on their surface. So, before the electrochemical studies, they were kept in an *aqua regia*

solution, for 4 h, to dissolve all the unwanted brazing material. Then, the tool bits were cleaned by ultrasounds, for 30 min, using deionized water. Fig. 1 shows the digital image of various WC-Co scraps.



Figure 1. Digital image of different forms of cemented WC-Co scraps for recycling: (a) scraps of crown bits; (b) corroded steel crown; (c) WC inserts; (d) WC scraps; (e) scraps of saw blades, broach cuttings, and drilling tools with a slight braze; and (f) heavily damaged WC buttons scraps.

The digital image of the as-received WC-Co scrap materials used in the present study is shown in Fig. 2.

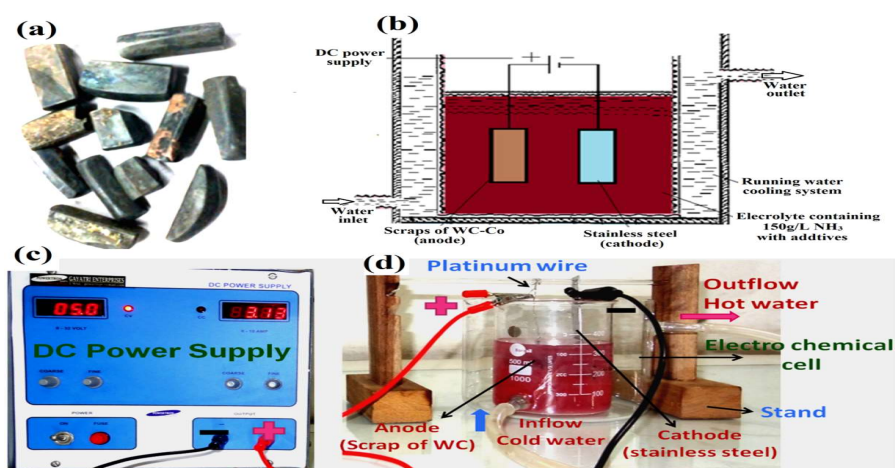


Figure 2. (a) Scraps of the cemented WC materials: the unwanted brazing material (golden-yellow) can be seen on its surface; (b) schematics of the electrochemical cell set up; (c) digital images of DC power supply; and (d) electrodisolution experiment cell set up equipped with a water recirculation system through annulus, for electrolyte cooling.

The cemented WC scrap sample contained 81.2% W, 5.2% C, 10.15% Co, 0.98% Fe, 0.062% Al and 0.005% Ti (all in wt.%). W, Co, and C are the major constituents in WC-Co. Impurities, such as Al, Ti and Mo, were present in trace amounts, including about 1.0% Fe.

The XRD pattern of the sample is shown in Fig. 3(e). The XRD peaks showed that the major phases were WC, Co₆W₆C and Co (JCPDS files: 25-1047, 23-0939 and 05-0727, respectively).

Chemicals

The NH₃ electrolytes were prepared by proper dilution of an AR grade NH₃ solution. All the dilutions were done using laboratory-grade deionized water processed by the Millipore Mili-Q system. The AR grade NH₄Cl, (NH₄)₂CO₃ and (NH₄)₂SO₄ were used as additives in the PDP and electrodisolution studies. All the abovementioned substances were procured from Merck Specialities Private Limited (Mumbai).

Electrodisolution methods

Initially, the WC-Co sample was subjected to PDP tests, so as to obtain an electrochemical response (dissolution and passivation), using a Gamry Echem Analyst potentiostat. WC-Co dissolution was subsequently studied by electrodisolution experiments, with the help of an electrolytic cell, by turning the sample into an anode in an electrochemical cell. A rectifier supplied the DC, procured from M/s Gayatri Enterprises, Pune. W and Co dissolved in the electrodisolution experiments were recovered by the precipitation method. Details of all the experimental procedures are given in the following sections.

PDP studies

A Gamry Echem Analyst potentiostat was used for PDP studies. A three electrode cell setup comprised WC-Co scraps, SC and a Pt foil, which were used as WE, RE and CE, respectively. The WE was connected, with the help of the Pt wire, to the power supply. The exposed surface area of the WC-Co sample was ~1cm², and it was coated with the chemically inert resin. The sample was polished so as to produce a new mirror surface, with the help of different grits of emery paper and a polishing disc, and rinsed with deionized water, before each experiment. The working cell consisted of a 150 mL glass beaker containing 100 mL of an electrolyte solution, WE (WC-Co scraps) and CE. This cell was filled with fresh electrolytes for each PDP experiment. The SC RE was placed in another glass beaker (reference cell) containing a 100 mL saturated KCl solution. A salt bridge was used to connect both cells.

To prepare a salt bridge, 2.5 gm agar-agar were thoroughly mixed into a solution of 25 g KCl in 150 mL deionized water, and heated at 90 °C. After mixing, the solution was partially cooled and sucked through one end of a 'U' shaped glass tube (salt bridge), until it reached the other end. The salt bridge was stored by dipping both ends in a saturated KCl solution in a glass beaker. During PDP studies, one end of

the salt bridge was placed close to the WE, while the other was placed near the RE [17]. In the PDP study, the applied E was increased with a programmed SR, while the current was continuously monitored. Then, J vs. applied E was drawn. Such as in a typical PDP scan, the initial and final E were set from -1.5 V to 7 V, with respect to the RE, at a SR of 1.5 mV/s. All the PDP experiments were carried out at room temperature. In some of them, the calculated quantity of a few chemicals was dissolved as an additive into the electrolyte, before the scan.

Electrodissolution studies

Electrodissolution experiments of the WC scraps were carried out in a 500 mL glass beaker cell. The cell, filled with 275 mL of electrolyte, was equipped with a water recirculation system, in order to cool the electrolytes during electrodisso- lution. WC scraps were connected to the Pt wire, and suspended in the electrolyte, as the anode. A 304 grade SS sheet was employed as cathode. Both anode and cathode were immersed into the electrolyte solution, and DC power was supplied by a rectifier manufactured by Gayatri Enterprises, Pune (model: Power Tron). In the electrodisso- lution experiments, the WC anode was connected to a positive power supply, and the negative power supply was connected to the SS cathode. In all the tests, there were efforts to control the cooling water temperature, by recirculation. During electrodisso- lution, the E (from 5 to 15 V) was applied by the rectifier, and the corresponding dissolution current was manually noted every 5 min, and the changes in temperature were measured by a thermometer.

Three sets of electrodisso- lution experiments were carried out, so as to obtain optimal conditions. In the first, different additives (NH_4Cl , $(\text{NH}_4)_2\text{SO}_4$ and $(\text{NH}_4)_2\text{CO}_3$) were taken (5% w/v) in 150 g/L NH_3 , at an applied potential of 10 V, to see their effect on J, and on W and Co recovery. The second set of experiments aimed to evaluate the impact of different NH_3 concentrations (100, 150 and 200 g/L) in 5% NH_4Cl , at an applied E of 10 V. The third set of experiments was run by varying the applied E (5, 10 and 15 V) and the additive concentrations (2, 5, 10 and 15% w/v) in a 150 g/L NH_3 electrolyte.

It is worth mentioning that all the electrodisso- lution experiments were carried out during 2 h. After each investigation, the cathode and anode were rinsed in the deionized water, dried in the air for 1 h, and weighed in an electronic balance, so as to calculate the anodic dissolution and cathodic deposition percentages, using the following formulas:

$$\%Dissolution = \frac{W_a - w_a}{W_a} \times 100 \quad (1)$$

$$\%Deposition = \frac{w_{cf} - w_{ci}}{W_a - w_a} \times 100 \quad (2)$$

where W_a and w_a are the weight (grams) of the anode (WC sample), before and after the experiment, respectively, and w_{ci} and w_{cf} are the initial and final weight (grams) of the cathode. After the experiments, the electrolyte was analyzed, in order to

determine W and Co concentrations. It is worth mentioning that each electrochemical measurement was performed four times, so as to ensure the repeatability of the experiments.

Characterization

The distribution of the samples morphology and surface elements was studied by SEM (Hitachi-S3400N scanning electron microscope), coupled with EDX. XRD patterns of WC-Co scraps and obtained WO_3 powder were recorded on a Siemens D500 X-ray diffractometer, using Ni filtered CuK_{α} radiation (30 kVA, 15 mA), at a scanning speed of $2^{\circ}(2\theta)/\text{min}$. The different phases were identified from the XRD pattern, with the help of JCPDS files.

Observation of the dissolved WC-Co scraps was also performed using AFM, so as to study the extent of the typical dissolution behaviour and explain its mechanisms, using the topographic image of the attacked surface, after the PDP and electrodisolution experiments. In order to study the surface characteristics, dissolved WC-Co samples were subjected to ultrasonic cleaning using acetone, for removing the loosely bounded undissolved and passivated materials from the anode surface. All the topographical studies were carried out in the contact mode, with asylum research AFM (MFP3D), at a SR of 0.5 Hz.

WO_3 recovery from the electrolytic solution

After the WC-Co dissolution, the concentrations of W, Co and other elements were estimated by ICP-OES. The spectrometer was calibrated using different dilutions of an individual analyte standard solution procured from Merck, India. After that, the samples were run through a capillary into the ICP, so as to determine the emission, which was automatically processed by the spectrometer, giving a final concentration value of a particular analyte.

The electrolyte obtained after the optimum electrodisolution experiment was further processed, in order to recover dissolved W as YTO. 50 mL of concentrated HCl were added drop by drop to the electrolyte containing $H_8N_2O_4W$ (Fig. 13), by constant stirring it, which produced a white milky solution. After HCl addition, the white solution was heated at $50\text{ }^{\circ}\text{C}$, for 1 h, for obtaining a yellow color precipitate of H_2WO_4 (Fig. 13(b)), which was separated by a centrifuge (5000 rpm). The yellow H_2WO_4 precipitate was heated for 1 h, at $900\text{ }^{\circ}\text{C}$, in a muffle furnace, so as to obtain YTO, which was subjected to XRD analysis.

Results and discussions

WC-Co scraps characterization

The scraps chemical composition was: 81.2% W, 5.2% C, 10.15% Co, 0.98% Fe, 0.062% Al, and 0.005% Ti (all in wt.%). W, Co, and C were the principal constituents in the WC-Co tool bits. However, the impurities (Al, Ti and Mo) were also present in trace amounts, including about 1.0% Fe.

In order to remove the brazed material, WC-Co scraps were dipped into the *aqua regia* solution, for 4h, at 50 °C. The samples were then cleaned, for performing the microstructural and XRD analyses. Fig. 3 (a) shows the micrographs of the WC-Co scraps in the BSE mode. Grey-colored fragmented WC grains were observed in the dark-colored Co matrix.

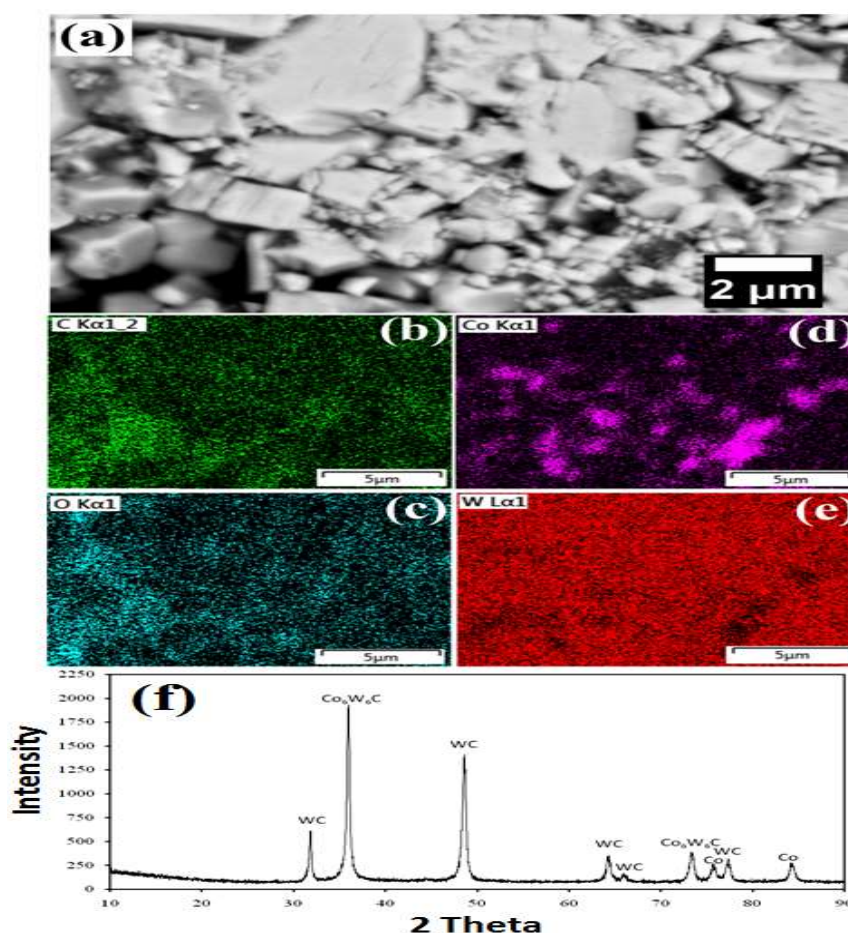


Figure 3. WC-Co scraps: (a) as-received microstructure; (b-d) mapping analysis after dissolution; and (e) XRD pattern.

The WC-Co tool bit was scrapped material obtained from mining sites. Since tool bits (as-received) faced extreme environmental conditions, fragmented WC grains were observed in the Co matrix. Different shapes and sizes and disintegrated small WC grains are shown in Fig 3(a).

Mapping results have confirmed the presence of various elements (O, C, W and Co) in the materials. The EDS map shows the homogeneous distribution of all the elements (Fig. 3(b-e)). The sample XRD pattern is shown in Fig. 3(f). XRD peaks showed that the major phases were WC (JCPDS file: 25-1047), Co₆W₆C (JCPDS file: 23-0939) and Co (JCPDS file: 05-0727).

PDP tests

The anode dissolution extent, its inherent mechanisms and passivation behavior can be well understood with the help of polarization tests, in terms of the OCP (Table 2) and J values (Fig. 4). The OCP value gives information about the thermodynamic stability or nature of the very thin passive film (EDL) formed at the WC-Co and NH₃ solution interface. However, maximum anodic J and OCP higher negative values provide useful information about the active dissolution reaction, rather than about passivation. It is worth mentioning that the OCP value was obtained after 1 h of exposure tests (Table 2). Therefore, the EDL was formed at the electrode/electrolyte interface. Consequently, all samples have been polarized from the OCP value.

Table 2. Various electrochemical parameters obtained after PDP tests.

NH ₃ solution	Additives types and amount	OCP	Maximum anodic J	Voltage corresponding to maximum anodic J
g/L	wt. %	mV _{SCE}	mA/cm ²	V _{SCE}
50	-	-824±12	20.30±0.35	2.50±0.047
100	-	-854±07	25.80±0.46	2.50±0.027
150	-	-884±16	32.80±0.15	2.50±0.044
150	1% (NH ₄) ₂ CO ₃	-719±12	294.40±0.62	4.78±0.035
150	1% (NH ₄) ₂ SO ₄	-779±11	352.40±0.83	3.43±0.047
150	1% NH ₄ Cl	-795±14	543.70±0.082	2.47±0.093
150	5% NH ₄ Cl	-659±08	819.10±0.063	2.03±0.038
150	10% NH ₄ Cl	-644±07	819.10±0.045	1.98±0.063

The OCP values increased with higher NH₃ solution concentrations (50, 100 and 150 g/L), because the tendency to dissolve WC-Co materials was higher in 150 g/L NH₃. Also, the pseudo-passive plateau region (from -1 to 1 V_{SCE}) has been observed for the 150 g/L NH₃ solution, indicating an active dissolution tendency (Fig. 4(a)).

However, in the 50 and 100 g/L NH₃ solution, a stable passive region could be seen in the same potential range (-1 to 1 V_{SCE}), showing the regular passive tendency on the WC-Co electrode surface. The anodic J values of the 50 and 100 g/L NH₃ solutions, at the same E range, were observed to be lower than that of the 150 g/L solution. This means that higher concentrations (150 g/L) of the NH₃ solution inhibited the passivation tendency.

Maximum anodic J at minimum E is a favored condition to achieve higher anodic dissolution rates, which is only possible by avoiding the anode passivation, with a higher NH₃ solution concentration (Fig. 4(a)).

Hence, maximum anodic current led to the maximum dissolution rate of WC-Co samples [17, 38]. However, the overall maximum anodic J was significantly lower in the NH₃ solution without additives, and further increase in the E may have strengthen the anodic current. Still, it would consume more energy, and increase the probability of formation of a passive oxide layer on the electrode surface.

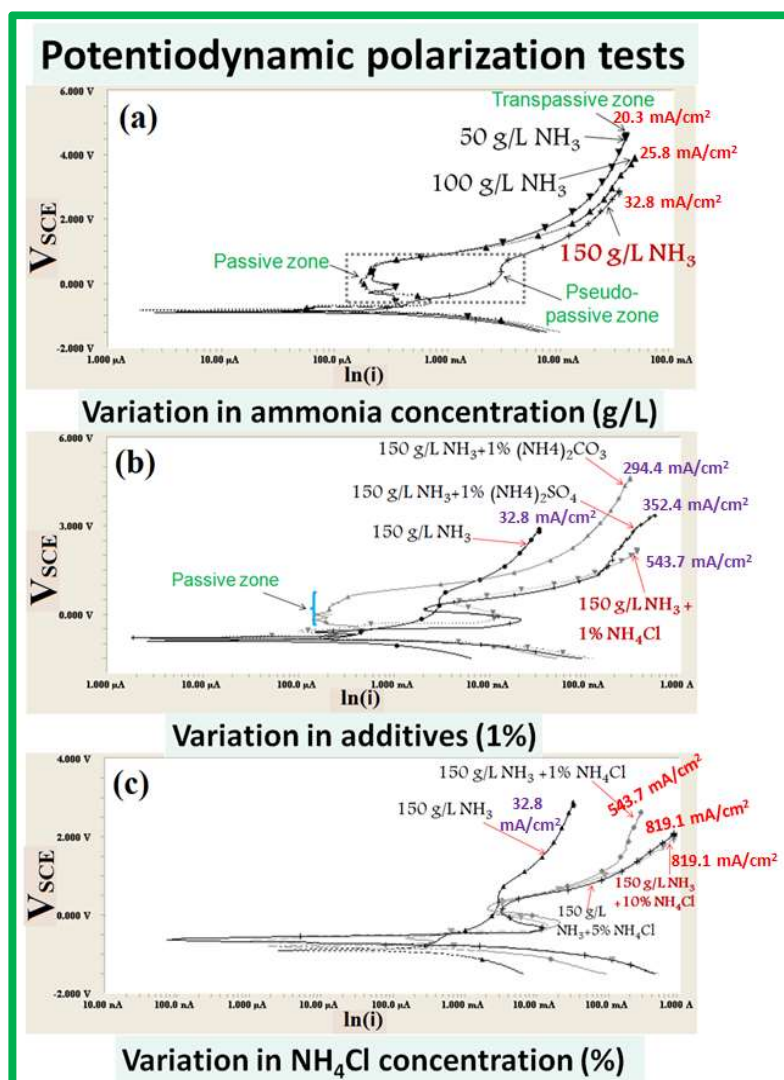


Figure 4. PDP tests of the WC-Co scraps in a freely aerated NH₃ medium with different additives: **(a)** 50, 100 and 150 g/L NH₃; **(b)** 150 g/L NH₃ + 1 % (NH₄)₂CO₃, (NH₄)₂SO₄, and NH₄Cl; and **(c)** 150 g/L NH₃ + 1, 5 and 10% NH₄Cl.

Therefore, the addition of chemical additives can avoid the formation of any passivation (Fig. 4(b)). Nevertheless, the NH₃ solution was initially not enough conducting to conduct the dissolved ions fastly in between the electrode. Thus, the dissolution rate was found to be very low, due to decreased anodic J.

The addition of compounds, such as NH₄Cl, (NH₄)₂SO₄ and (NH₄)₂CO₃, has not only contributed to increase the solution conductivity (by adding the additional ions), but has also avoid the possibility of any stable passive film formation on the WC-Co materials exposed surface (Fig. 4 (b and c)).

When it is likely that a stable passive layer is formed, the Cl⁻ ions turn out to be highly aggressive, and penetrate through it, by attacking W and Co (which is responsible for local passivation), forming complex products and decreasing the

possibility of the layer formation. Similarly, SO_4^{2-} and CO_3^{2-} have done the same thing, but they were less effective than Cl^- ions [39].

Therefore, such additives (containing aggressive ions) decreased the possibility of a stable passive layer being formed, and the resultant maximum anodic dissolution current was obtained at minimum E (Table 2).

However, WC dissolution was still hindered by the same optimal concentration of 150 g/L NH_3 solution, with 1% NH_3 Cl additives (Fig. 4(b)). So, an increase in NH_4Cl up to 10 %, in a 150 g/L NH_3 solution, enhanced the anodic dissolution.

SO_4^{2-} and CO_3^{2-} have a similar behaviour, but they are less effective than the Cl^- ions [39].

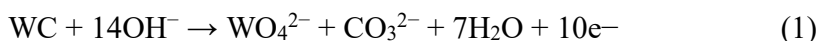
In summary, if the NH_3 solution concentration increases from 50 to 150 g/L, the corresponding OCP value decreases. This means that the NH_3 concentration makes the surface thermodynamically more active for dissolution, while the anodic current drops, because Co tries to passivate the surface in the absence of these aggressive ions, by forming a stable complex (Fig. 4(c)).

Furthermore, a more negative OCP value (Table 2) represents a higher tendency for WC dissolution in NH_4OH . This indicates that NH_3 concentrations can limit the anodic dissolution rate. However, the OCP values were still very low, even after the addition of 1% NH_4Cl , $(\text{NH}_4)_2\text{SO}_4$ and $(\text{NH}_4)_2\text{CO}_3$. Moreover, OCP tended to shift towards the noble direction, with 1 to 10% NH_4Cl . It is interesting to note that this behavior was not maintained in the presence of Cl^- ions (after the addition of 5 to 10% NH_4Cl), which probably reduced the tendency for a passive layer being formed on the exposed surface. Thereby, a stronger dissolution tendency has been observed at higher concentrations (150 g/L NH_3 with 10% NH_4Cl) of Cl^- ions, at minimum E.

Hence, it is inferred that the additives played a significant role in the WC materials de-passivation, and in the solution conductivity increase. However, W driving force and maximum solubility limit, in the NH_3 solution fixed concentration, became a rate-limiting step for WC-Co dissolution. This could explain why OCP value has shifted towards a noble direction, even after the addition of 1% NH_4Cl , $(\text{NH}_4)_2\text{SO}_4$ and $(\text{NH}_4)_2\text{CO}_3$, and an increase in the NH_4Cl additives concentration, from 1 to 10%. Since the electrolyte volume (100 mL) was fixed in all polarization tests, the same J value (819.1 A/cm^2) has been noticed at different NH_4C concentrations (5 and 10 %). However, the applied E was lower (1.98 V_{SCE}), in the case of 10% NH_4Cl . Although the OCP value has shifted to a noble direction, WC-Co dissolution tendency could be strongly limited by the NH_3 solution concentration (without agitation). Also, maximum J value has been similarly obtained, because Co could not form a passive film on the surface, due to a high concentration of Cl^- ions (in both cases).

In general, W was more anodically active in the NH_3 medium than Co. Thereby, the formation of a W-based passive layer is less probable than that of Co, with higher NH_3 concentrations. Hence, once the maximum Cl^- ions concentration was reached (in the same volume of the NH_3 solution), Co also ceased being able to form a passive layer, due to their aggressive nature. Therefore, the anodic J value has reached its maximum value at the minimum E.

During the electrodisolution experiments, the WC-Co dissolution progressed, by forming WO_4^{2-} and Co^{2+} . However, W standard dissolution or oxidation E (0.09 V) was lower than that of Co (0.28 V). Hence, W tended to dissolve first, forming WO_4^{2-} ions. And then, the anode became passivated when E reached a higher value, due to Co dissolution and formation of a passive layer [40]. Therefore, W formed WO_4^{2-} , through the anodic oxidation reaction in the NH_3 solution, or due to the NaOH solution high pH (~11). Further, WO_4^{2-} reacted with NH_4^+ , which is the soluble product, and the following chemical reaction can be expected [39, 40].



The formation of WO_4^{2-} was thermodynamically more feasible with a higher NH_3 concentration (150 g/L), at a given E range. Hence, this reaction moved forward, and became more thermodynamically active when the NH_3 content increased.

On the other hand, the Co binder anodic dissolution also occurred through the oxidation reaction, by forming Co^{2+} . However, these tended to form a Co-based amine complex. Co has a higher tendency to form an octahedral amine-based complex ($[\text{Co}(\text{NH}_3)_6]^{+2}$), at a high dissolution E (0.28 V), in which NH_3 acts as a ligand, and the following reaction can be expected [41]:

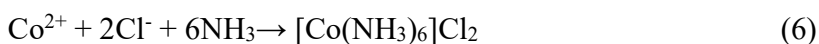


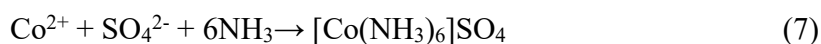
Although Co^{2+} can be passivated by forming Co-hydroxides, which hinders further oxidation, this reaction depends on the NH_4OH concentration that WO_4^{2-} ions can also consume, and the following reaction is expected to occur:



This concentration (150 g/L) and the NH_3 solution pH (~11) significantly affected the WC-Co surfaces dissolution and passivation tendency. However, the Co^{+2} oxidation E was very high (0.28 V). Hence, at higher E and pH values, $[\text{Co}(\text{NH}_3)_6]^{+2}$ complex became more stable than Co^{3+} , which is also relatively stable at lower pH values [41]. Hence, at higher E and low pH (~ 7) values, Co^{+2} ions also oxidized into the very low oxidation E of Co^{+3} ions (-1.82 V), forming the unstable amine-based complex $[\text{Co}(\text{NH}_3)_6]^{+3}$ [39].

150 g/L NH_3 with the aggressive anions Cl^- , SO_4^{2-} and CO_3^{2-} (separately obtained in the presence of NH_4Cl , $(\text{NH}_4)_2\text{SO}_4$, and $(\text{NH}_4)_2\text{CO}_3$.) have significantly influenced the abovementioned reaction, by avoiding the stable Co passive layer formation. Therefore, enhanced anodic current was due to the higher anodic dissolution, by the formation of $[\text{Co}(\text{NH}_3)_6]\text{Cl}_2$, $[\text{Co}(\text{NH}_3)_6]\text{SO}_4$ and $[\text{Co}(\text{NH}_3)_6]\text{CO}_3$ complexes, and the following chemical reaction can be expected [39].





WC-Co dissolution mechanisms

After the PDP tests, the AFM micrographs were used to obtain the dissolution behavior of the polarized WC-Co surface, which was caused by the aggressiveness of the different concentrations of NH_3 electrolytes with various additives. The AFM topographical micrographs from the corroded WC-Co surface helped to examine the anode materials dissolution tendency, based on the average R_a . The dissolution intensity, which is a localized attack on the polarized surface, can vary accordingly to different conditions, which depend on the ions (Cl^- , SO_4^{2-} and CO_3^{2-}) aggressiveness, and on the correspondingly obtained maximum anodic J . Hence, the attacked surface was evaluated after the PDP tests, in terms of the average R_a value. Fig. 5 shows the WC-Co anode topographical image, after electrochemical dissolution tests in a freely aerated 150g/L NH_3 solution with 1% $(\text{NH}_4)_2\text{CO}_3$.

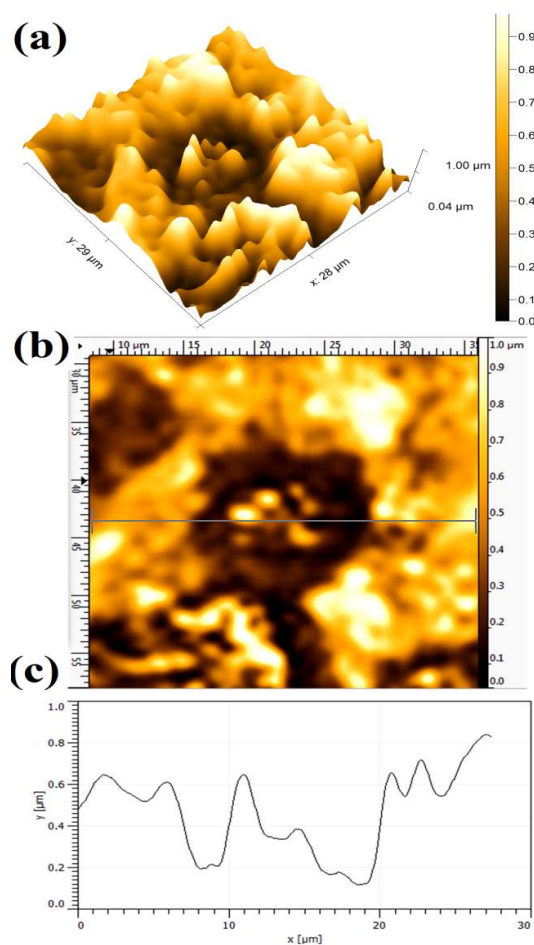


Figure 5. Topographical image of WC-Co anode, after PDP tests, in a freely aerated 150 g/L NH_3 solution with 1% $(\text{NH}_4)_2\text{CO}_3$.

A more severe dissolution can be seen at the WC grains and Co matrix interface. Since the WC grains are nobler than the Co matrix, maximum dissolution can be seen in the binder phase (Co) regions. The dissolution differential that occurs between the WC grains and the Co electrode is due to their different E values, which lead to the cathode and anode formation. Hence, the dissolution behavior is mainly influenced by the formation of galvanic couples between the WC grains noble cathode and the Co phase active anode [2, 42]. The average R_a value was $0.387 \pm 0.017\mu\text{m}$, in the presence of $(\text{NH}_4)_2\text{CO}_3$ additives.

Fig. 6 shows the WC-Co anode topographical image, after the electrochemical dissolution tests, in a freely aerated 150g/L NH_3 solution with 1% $(\text{NH}_4)_2\text{SO}_4$. The average R_a was obtained at $0.503 \pm 0.013\mu\text{m}$. However, the dissolution behavior was identical.

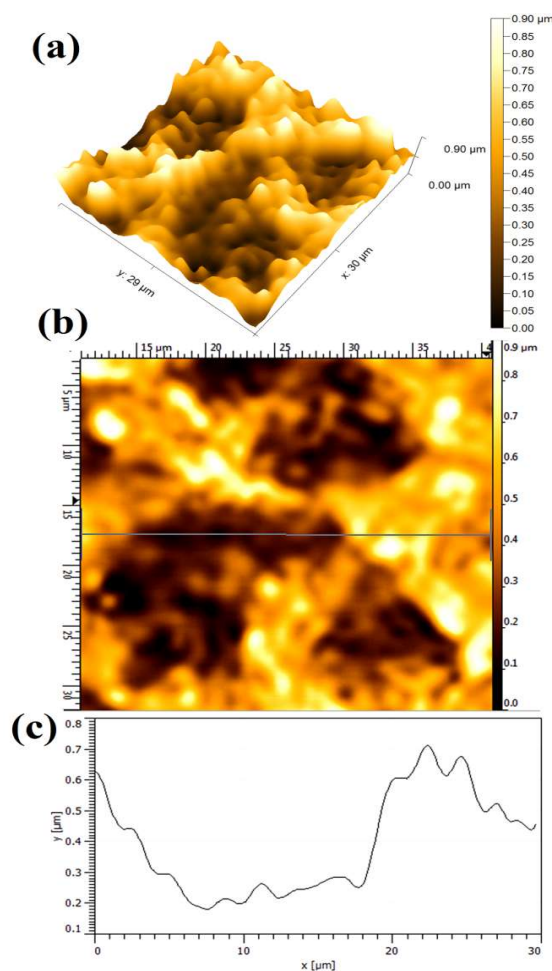


Figure 6. Topographical image of WC-Co anode, after PDP tests, in a freely aerated 150 g/L NH_3 solution with 1% $(\text{NH}_4)_2\text{SO}_4$.

Fig. 7 shows the WC-Co anode topographical image, after electrochemical dissolution tests, in a freely aerated 150g/L NH_3 solution with 1% NH_4Cl . The lowest ($0.387 \pm 0.017\mu\text{m}$),

intermediate ($0.503 \pm 0.013 \mu\text{m}$) and highest ($0.704 \mu\text{m} \pm 0.083 \mu\text{m}$) R_a values were obtained with 1% each $(\text{NH}_4)_2\text{CO}_3$, NH_4Cl and $(\text{NH}_4)_2\text{SO}_4$, respectively.

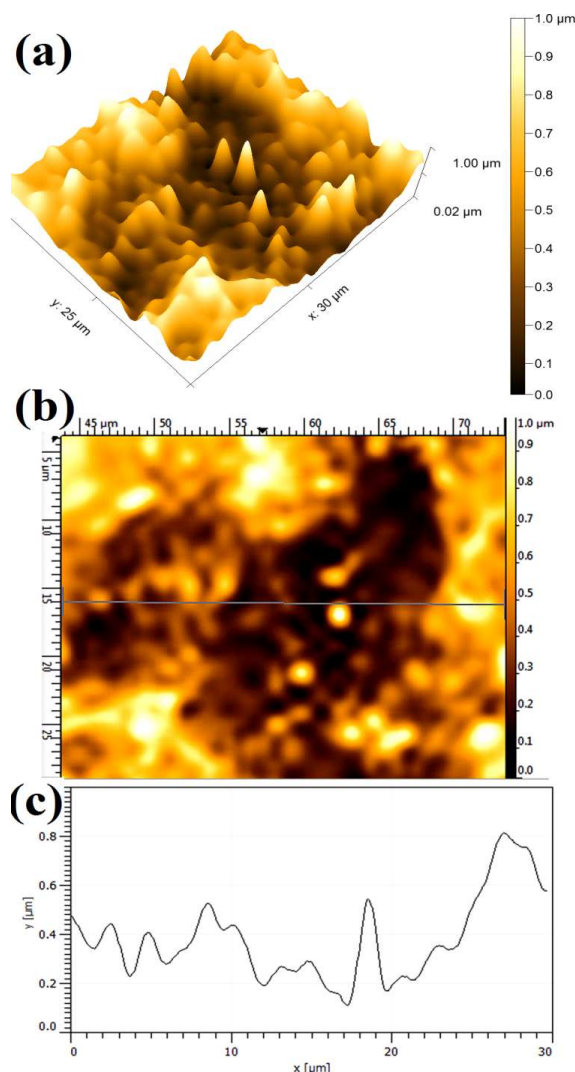


Figure 7. Topographical image of WC-Co anode, after PDP tests, in a freely aerated 150 g/L NH_3 solution with 1% NH_4Cl .

Fig. 8 shows the polarized WC-Co anode topographical image in a 150 g/L NH_3 solution with 5% NH_4Cl . Since the maximum dissolution current was observed in the presence of 5% NH_4Cl additives, it can be seen in terms of the average R_a value ($0.842 \mu\text{m} \pm 0.051 \mu\text{m}$). The stronger attack led to WC-Co maximum dissolution depth, which resulted in a rougher surface, and in its limited tendency to form an adherent or protective layer on the anode surface. In fact, the formation of a stable passive layer can reduce the dissolution attack, in the presence of $(\text{NH}_4)_2\text{CO}_3$ and $(\text{NH}_4)_2\text{SO}_4$ additives. Therefore, the anode susceptibility to dissolution, with

different additives in the NH_3 solution, is strongly influenced by the obtained maximum anodic J and the presence of different ions.

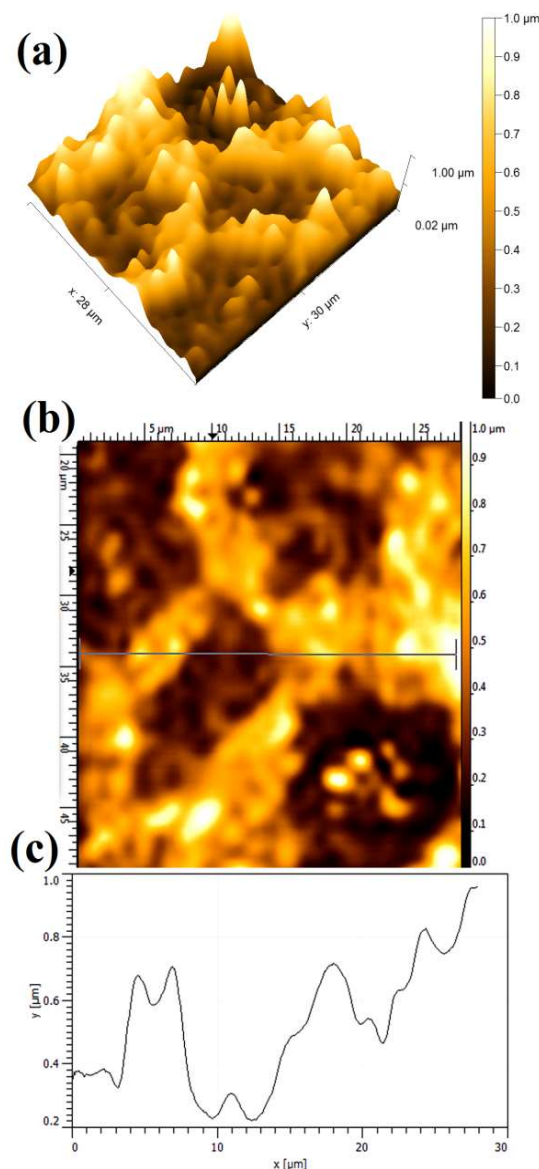


Figure 8. Topographical image of WC-Co anode, after PDP tests, in a freely aerated 150 g/L NH_3 solution with 5% NH_4Cl .

WC-Co electrodisolution tendency

Combined effect of NH_3 and additive concentrations

It is worth mentioning that the time of all the electrodisolution experiments was exactly 2 h, and the electrolyte was at ambient temperature. Co cathodic deposition, and the average anodic J obtained after the WC-Co scraps dissolution in freely aerated solutions, using different parameters, are given in Table 3.

Table 3. Co cathodic deposition and average J obtained after WC-Co scraps dissolution in freely aerated solutions, using different parameters.

Additives	WC-Co dissolution	Cathodic deposition	Average J
Different concentrations of the NH₃ solution (g/L) with 5% NH₄Cl.			
Time: 2 h. Potential: 10 V. Temperature: ambient.			
100 g/L	22.53±1.32	7.77±1.35	0.379±0.018
150 g/L	23.54±2.43	11.72±1.75	0.599±0.047
200 g/L	37.4±3.51	4.51±2.09	0.469±0.037
150 g/L NH₃ solution with 5% different additives.			
Time: 2 h. Potential: 10 V. Temperature: ambient.			
5%	17.37±1.02	4.55±0.74	0.298±0.045
5%	20.85±1.73	5.70±1.03	0.290±0.089
5% NH₄Cl	23.54±2.43	11.72±1.75	0.599±0.047
150 g/L NH₃ solution containing different amounts of NH₄Cl.			
Time: 2 h. Potential: 5 V. Temperature: ambient.			
2% NH₄Cl	5.32±0.86	4.357±1.05	0.094±0.004
5% NH₄Cl	13.96±1.86	1.434±0.79	0.159±0.009
10% NH₄Cl	16.35±2.05	0.858±0.54	0.233±0.084
15% NH₄Cl	26.92±3.76	0.777±0.25	0.339±0.095
150 g/L NH₃ solution containing different amounts of NH₄Cl.			
Time: 2 h. Potential: 10 V. Temperature: ambient.			
2% NH₄Cl	18.76±1.56	10.31±2.42	0.429±0.085
5% NH₄Cl	23.54±2.43	11.72±1.75	0.599±0.047
10% NH₄Cl	27.64±3.24	9.5±1.92	0.866±0.098
15% NH₄Cl	48.37±5.06	6.9±1.24	1.661±0.127
150 g/L NH₃ solution containing different amounts of NH₄Cl			
Time: 2 h. Potential: 15 V. Temperature: Ambient			
2% NH₄Cl	41.46±5.28	7.5±1.45	0.534±0.028
5% NH₄Cl	49.86±6.17	7.9±1.07	1.079±0.054
10% NH₄Cl	51.10±7.63	7.0±1.31	1.507±0.097

However, electrodisolution studies in the NH₃ medium without additive were not carried out, since PDP studies without an additive gave rise to a much weaker anodic current. Therefore, a study in the NH₃ medium (150 to 200 g/L) with 5% NH₄Cl additives was performed, to ensure the active dissolution and the deposition effect with the solution higher concentrations.

It can be seen, from Fig. 9(a), that the anodic dissolution that was achieved at a NH₃ concentration of 200 g/L, was the highest, while the cathodic one was the lowest. This was perhaps because some loosened anode material, caused by Co partial dissolution, settled at the bottom of the electrolyte without being dissolved (later, it could be recovered by electrowinning methods). However, the highest J value was achieved with a 150 g/L NH₃ solution. Thus, this NH₃ concentration with 5% NH₄Cl was considered an optimum condition, and further experiments were carried out with this parameter. Fig. 9(b) also shows the correlation among the anode material (WC-Co tool bits) dissolution (%), Co deposition (%) at the cathode and average J, achieved by the electrodisolution experiments, in the 150 g/L NH₃ solution with 5% each of (NH₄)₂CO₃, (NH₄)₂SO₄ and NH₄Cl, at 10 V. Those parameters achieved their maximum values with 5% each NH₄Cl, followed by (NH₄)₂SO₄ and (NH₄)₂CO₃. The highest cathodic deposition (11.72%) and the maximum average J (0.5995 A/cm²)

were observed, because Cl^- ions accelerated the dissolution rate, by avoiding the passivation in the 150 g/L NH_3 electrolyte with 5% NH_4Cl . Therefore, it was found that NH_4Cl was the best option, and, hence, further experiments in the NH_3 medium were carried out only with this additive.

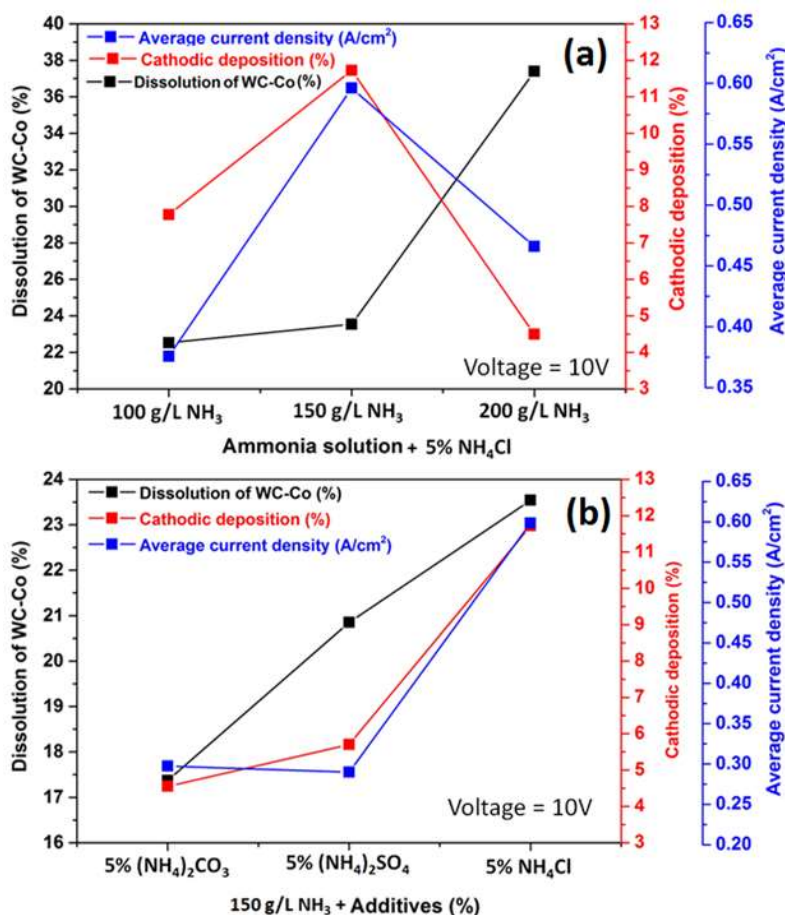
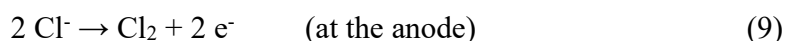


Figure 9. Correlation between the WC-Co scraps dissolution (%), Co cathodic deposition (%) and average J with: (a) different NH_3 concentrations (100, 150 and 200 g/L) with 5% NH_4Cl , at 10 V, at ambient temperature, for 2 h; and (b) with 5% of different additives ($(\text{NH}_4)_2\text{CO}_3$, $(\text{NH}_4)_2\text{SO}_4$, and NH_4Cl) in a 150g/L NH_3 solution, at 10 V, at ambient temperature, for 2 h.

During the studies on the NH_3 concentration effect on the WC-Co tool bits electrodisolution, it was observed that some Cl_2 evolution took place at the cathode, with the NH_3 lower concentrations (50 and 100 g/L), which may have influenced Co deposition behavior on the SS cathode. At higher NH_3 concentrations (150 and 200 g/L), no Cl_2 evolution was observed. It seems that, with higher NH_3 concentrations, whatever Cl_2 amount was evolved at the anode, in NH_4Cl electrolysis, got converted to HCl , which reacted with NH_3 , producing NH_4Cl [43].





NH₄Cl and impressed voltage synergistic effect

The effect of varied (2, 5, 10 and 15%) NH₄Cl amounts, in the 150 g/L NH₃ electrolyte, on the WC-Co tool bits electrodisolution, at 5, 10 and 15 V, is shown in Fig. 10 (a), (b) and (c), respectively. It can be seen that the electrodisolution was stronger as the NH₄Cl amount increased from 2% to 15%.

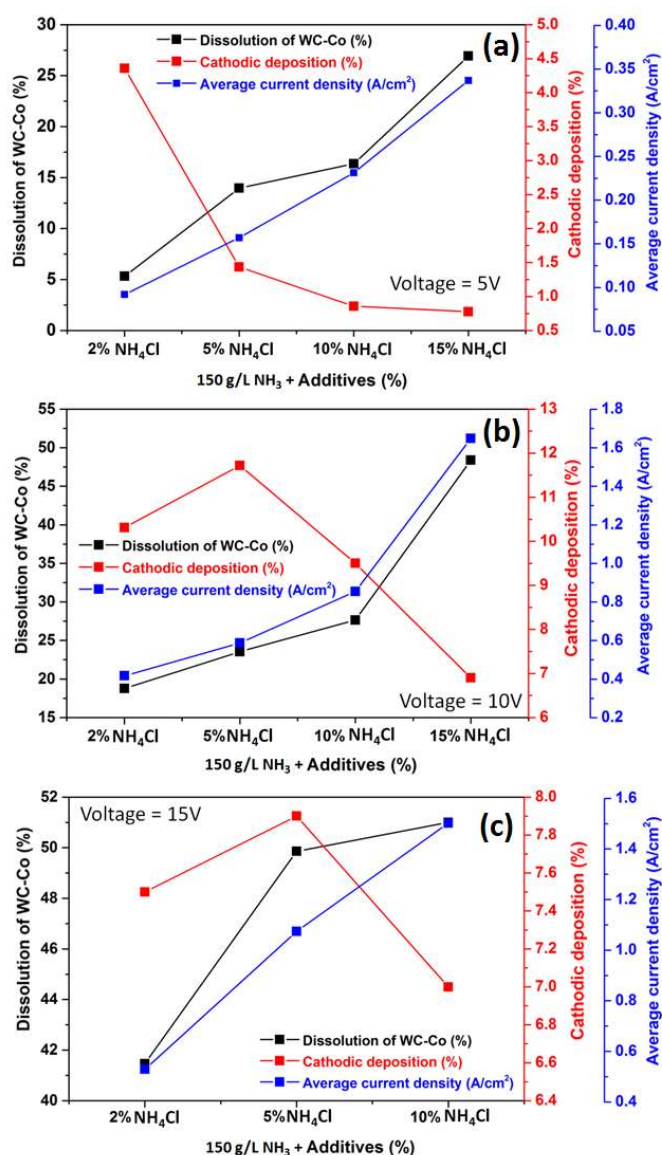


Figure 10. Correlation between WC-Co scraps dissolution, Co cathodic deposition (%) and average J, with 2, 5, 10 and 15 % NH₄Cl additives in a 150g/L NH₃ solution, at operating voltages of: (a) 5 V; (b) 10 V; and (c) 15 V, at ambient temperature, for 2 h.

Fig. 10 (a) shows the correlation among the WC-Co scraps dissolution (%), Co cathodic deposition (%) and average J values, with NH₄Cl different concentrations (%) in a 150g/L NH₃ solution, at an operating voltage of 5 V, at ambient temperature. It can be seen that the average J values increased with higher NH₄Cl amounts.

Additionally, the NH₃ electrolyte became more conductive with higher levels of Cl⁻ ions. The maximum dissolution achieved by the WC-Co tool bits was 26.92%, with 15% NH₄Cl, because the average anodic J increased with higher contents of this additive, from 2 to 15%, at 5 V.

The cathodic deposition values in these experiments are also plotted in Fig. 10(a), which shows that it decreased with higher additive amounts, reaching its maximum (4.36%) with 2% NH₄Cl.

The average J values with NH₄Cl different amounts, at 10 V, are plotted in Fig. 10(b). They were much higher at 10 V than at 5 V. Maximum J, with 15% of the additive, was 1.66 A/cm², at 10 V, while, at 5 V, it was 0.34 A/cm².

The effect of NH₄Cl addition, at this higher voltage, on the WC-Co tool bits dissolution (%) is shown in Fig. 10(b). It was seen that the anodic dissolution was stronger with increasing additive percentages, and maximum dissolution (48.3%) was obtained with 15% NH₄Cl.

It was observed that the maximum cathodic deposition (11.72%) was obtained with 5% of NH₄Cl, and, with higher percentages, it drastically decreased (Fig. 10 (b and c)), due to the formation of Cl₂ gas bubbles near the cathode.

The electrodisolution studies were carried out at higher voltage (15 V), with 2, 5 and 10% NH₄Cl. It can be seen, from Fig. 10(c), that the WC-Co tool bits anodic dissolution increased with higher NH₄Cl amounts. About 50% of the anode dissolution occurred with 5% NH₄Cl. With 10% NH₄Cl, the dissolution was just 51%. Therefore, experiments with higher NH₄Cl amounts were not carried out. The cathodic deposition values with different percentages of the additive, in the electrodisolution experiment, at 15 V, are shown in Fig. 10 (c). Here, the maximum cathodic deposition was achieved with 5% NH₄Cl. It is worth mentioning that the increase in voltage (10 to 15 V) with higher NH₄Cl percentages (10 to 15%) led to stronger anodic currents that caused the anode decomposition and fragmentation. Hence, less Co dissolution in an electrolyte may lead to lower deposition.

Fig. 11 shows that the average J values and corresponding WC-Co scrap dissolution increased at higher operating voltages, with concentrations of 2, 5 and 10% NH₄Cl. However, the cathodic deposition reached its maximum at 10 V, with those concentrations of the additive. Therefore, 5% NH₄Cl in the 150 g/L NH₃ solution, at 10 V, was an optimum parameter for WC-Co scraps dissolution (%), Co deposition on the cathode surface and average maximum J.

It is worth mentioning that all the electrodisolution studies have been carried out for two hours, and it is expected that, with a longer duration of the experiment, higher recovery could be achieved.

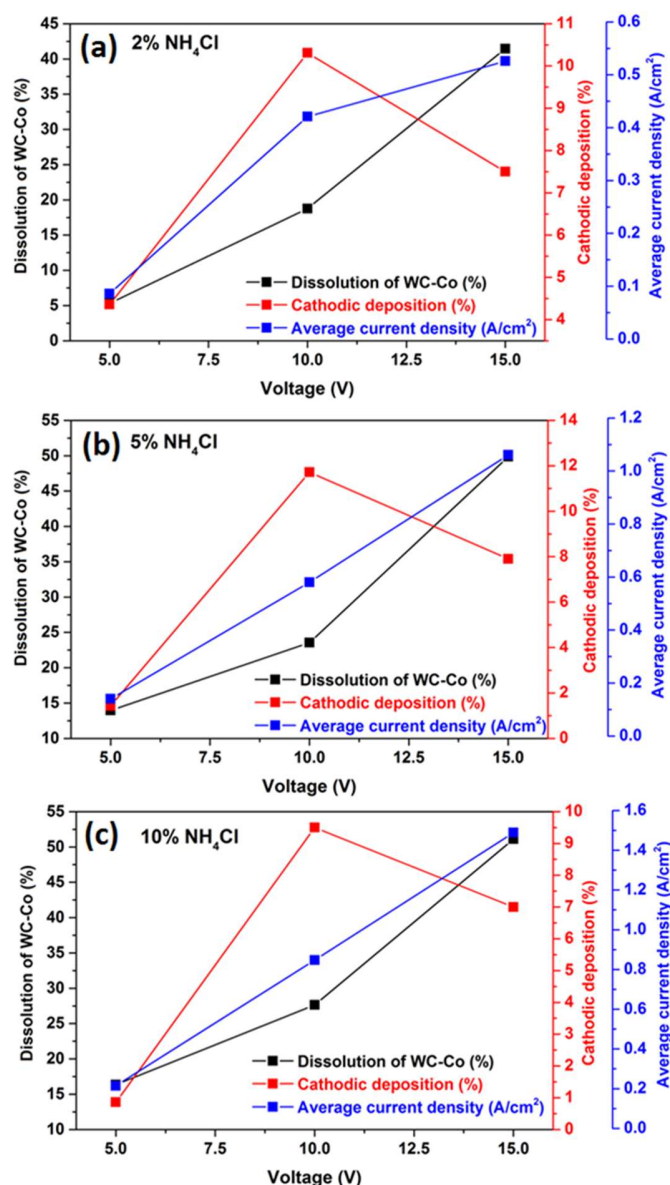


Figure 11. Correlation between WC-Co scraps dissolution (%), Co cathodic deposition (%) and average J with: (a) 2%; (b) 5%; and (c) 10% of NH₄Cl in a 150g/L NH₃ solution, at different operating voltages of 5, 10 and 15 V, at ambient temperature, for 2h.

Dissolved WC-Co surface morphology

Resuming, the optimum parameter for the stronger WC-Co scraps dissolution (%) and average maximum J was found to be with 15 % NH₄Cl in the 150 g/L NH₃ solution, at 10 V. The extent of WC-Co dissolution can be clearly observed by AFM micrographs. Fig. 7 shows the WC-Co anode materials topographical image after the electrochemical dissolution tests, in a freely aerated 150 g/L NH₃ solution with 15% NH₄Cl. The maximum average R_a value (1.82 ± 0.085 μm) was obtained. It is worth mentioning that, before the AFM analysis, the WC-Co remaining anode,

obtained after electrodisolution, was subjected to 20 min of ultrasonic cleaning, in an acetone medium, so as to remove its loosely bounded residues, and enhance the surface topography image.

Fig. 12 (a) shows the number of WC grains that were dissolved or coming out from the matrix. However, the dissolution could have started in the WC grains and Co interface. However, undissolved WC grains could also be seen after the Co phase dissolution.

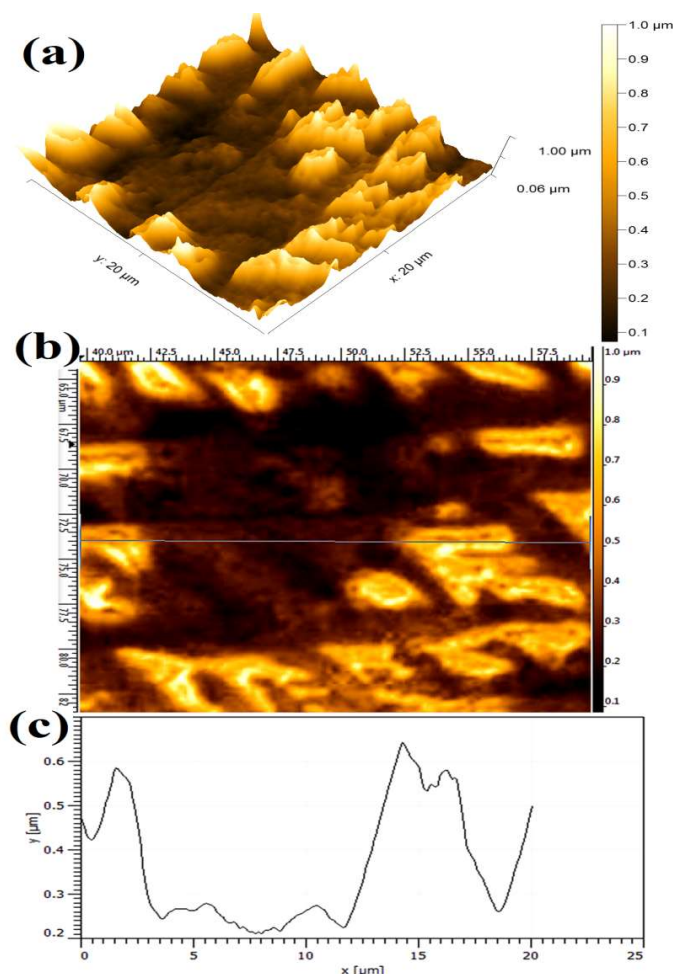


Figure 12. Topographical image of WC-Co anode, after electrochemical dissolution tests, in a freely aerated 150g/L NH_3 solution with 15% NH_4Cl , at 10 V.

W recovery from the electrolytic solution

W recovery in the electrodisolution experiments was calculated based on the anode chemical analysis and the metal dissolved in the electrolyte. The recovery values, at 5 V, with different NH_4Cl percentages, are given in Table 4. It can be seen that W recovery increased with higher NH_4Cl percentages, reaching a maximum value of 37.51% with 15% NH_4Cl . At 10 V, W recovery also increased with higher NH_4Cl

percentages in the 150 g/L NH₃ electrolytes, reaching a maximum value of 65.26% with 15% NH₄Cl.

Table 4. W recovery in the electrolyte, after the electrodisolution experiments.

Applied voltage (V)	150 g/L NH ₃ solution + % additives			
	2% NH ₄ Cl	5% NH ₄ Cl	10% NH ₄ Cl	15% NH ₄ Cl
5	8.69±1.31	20.82±2.42	23.62±2.43	37.51±3.76
10	17.92±1.86	25.31±1.86	35.45±1.45	65.26±7.63
15	61.10±4.28	69.72±6.06	68.53±5.28	-

With different concentrations of NH₄Cl in 150 g/L NH₃ electrolytes, W recovery in the electrodisolution was quite high, at 15 V. It was 61.10% with 2% NH₄Cl, and it increased to 69.72% with 5% NH₄Cl. With 10% NH₄Cl, there was no significant change in W recovery (65.53%). Since W recovery with 5 and 10% NH₄Cl was almost the same, no further experiments with higher amounts of the additive were made.

Although the highest W recovery in the electrodisolution study was obtained with 5% NH₄Cl, at 15 V, the electrolyte temperature increased more (75 °C) than at 10 V (45 °C). It may be noted that the experiments at 10 V yielded 65.1% of W recovery, with 15% NH₄Cl, which was very near to its highest amount (69.72%), at 15 V. However, since the electrodisolution at 10 V consumed less energy than at 15 V, it seems that the optimal parameters for WC-CO tool bits electrodisolution, were 10 V and 15% NH₄Cl in 150 g/L NH₃. W recovery in the electrolyte solution was 65.1%, for 2 h, and it was further treated to produce saleable YTO.

Products characterization

After the electrodisolution experiments, the NH₃ electrolyte containing W, as H₈N₂O₄W, was acidified with HCl and heated, for 1 h, at 50 °C. The precipitated H₂WO₄ was separated by centrifugation, and heated at 900 °C, to obtain YTO. An image of YTO prepared from WC-Co scraps is shown in Fig. 13.

Fig. 13(a) shows the H₈N₂O₄W solution obtained after the electrodisolution tests. Fig. 13(b) shows the precipitated H₂WO₄ obtained after the H₈N₂O₄W solution acidification. The acidification with HCl was followed by mild heating at 50 °C, for 1 h. Fig. 13(c) shows the YTO powder produced from the precipitated H₂WO₄ that was obtained after centrifugation, followed by heating at 900 °C, in a tube furnace. The purity of W and Co recovered from the WC-Co scraps was also a significant concern of the present study. Hence, YTO powder was also compared to the standard WO₃ XRD pattern, as shown in Fig. 13(d). The XRD pattern of the YTO prepared in the present work matched well with the standard WO₃ JCPDS pattern (43-1035) shown in Fig. 13(e), which confirmed the nature of the product. Co deposited on the cathode was manually separated and washed with deionized water, for the XRD characterization. A SEM image of Co cathodic deposition (inset of Fig. 13(f)), in the

form of separated chips, and the corresponding EDS spectra, are shown in Fig. 13(f) and (g), respectively.

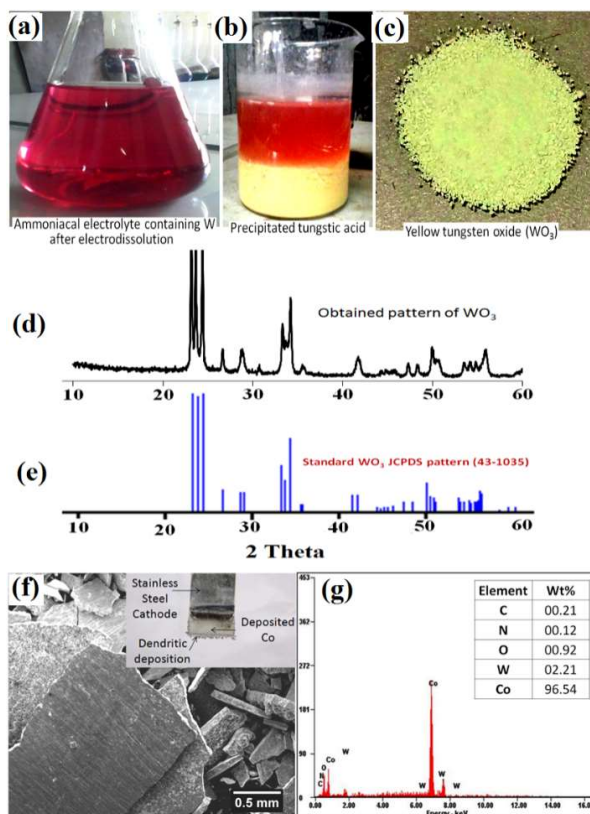


Figure 13. (a) Electrolyte after electrodisolution tests (pink colored $H_8N_2O_4W$ solution); (b) precipitated H_2WO_4 ; (c) YTO; (d) XRD pattern of YTO prepared in the present work; (e) YTO XRD pattern compared with that of JCPDS (43-1035); (f) SEM image of the deposited Co cathode after WC-Co scrap samples electrodisolution; and (g) EDS pattern of the deposited Co cathode.

In the present paper, PDP studies on WC-Co scraps have been carried out, since they reveal better their anodic dissolution behavior, in order to recover those metal values. PDP studies also provided information on suitable electrolytes, and found out the maximum anodic current at selective electrolytes, with or without additives. The maximum anodic current produced the WC-Co scraps stronger dissolution, without any passivation. During the electrodisolution experiments, it was initially found that the anodic current was very high, and, after some time, it continuously decreased, causing a reduction in the anode dissolution. This phenomenon is called passivation, and it occurred due to the formation of the anode passive layer. However, it was seen that the anodic passivation retarded the scraps dissolution, and adversely affected the metals recovery. So, in order to minimize the passivity and increase the anodic dissolution, some chemicals were used as additives. NH_4Cl ,

$(\text{NH}_4)_2\text{CO}_3$ and $(\text{NH}_4)_2\text{SO}_4$ were added in different concentrations to the NH_3 electrolyte. The studies revealed that 5% NH_4Cl were suitable for obtaining the maximum anodic dissolution (current) in 150 g/L NH_3 . Therefore, the WC-Co tool bits electro-dissolution in NH_3 effectively dissolved both W, as $\text{H}_8\text{N}_2\text{O}_4\text{W}$, and Co, as a Co-amine complex. Further, Co was deposited at the cathode during the electrolysis, while $\text{H}_8\text{N}_2\text{O}_4\text{W}$ remained in the electrolyte, from where W could be recovered as H_2WO_4 or WO_3 .

Therefore, WC-Co scrap produced by the mining industries was electrochemically dissolved, producing $\text{H}_8\text{N}_2\text{O}_4\text{W}$, and Co collected from the cathode. $\text{H}_8\text{N}_2\text{O}_4\text{W}$ was converted into APT crystal, by filtering and evaporating it into white APT. On the other hand, $\text{H}_8\text{N}_2\text{O}_4\text{W}$ electrolytes could be converted into W acid, by neutralization, using HCl, and later, they could be recovered in the form of YTO. Hence, the present recycling technique has more advantages than those from the reported recycling techniques, such as single-step direct processes, high purity saleable products (APT, WO_3 and Co), low energy consumption and low cost environmentally friendly recycling methods.

Process flowsheet

Based on the electro-dissolution studies, a flowsheet was proposed and illustrated (Fig. 14), for explaining the unit operations.

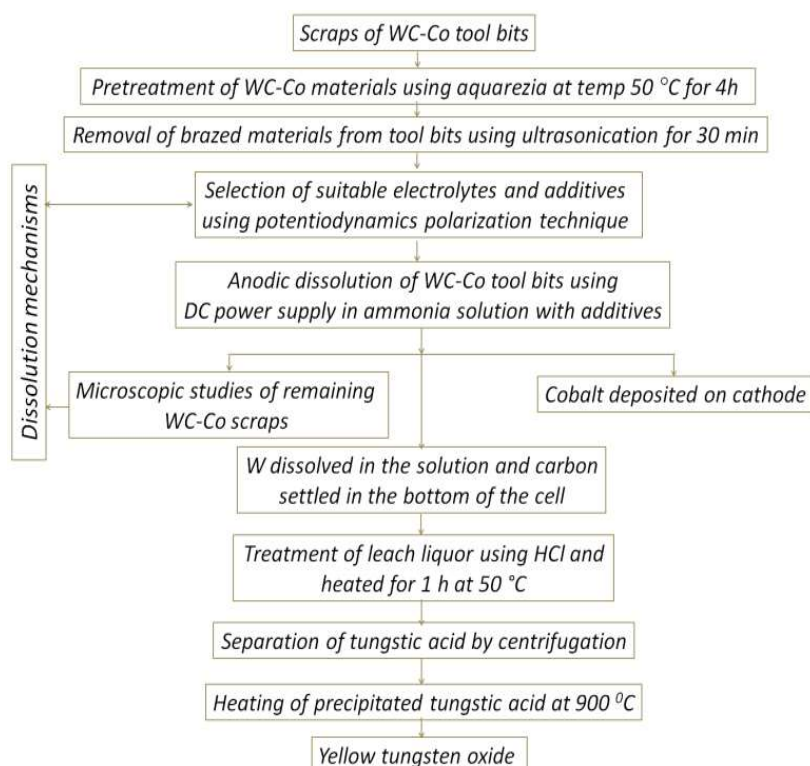


Figure 14. Flow chart for WC scraps recycling through electro-dissolution routes, and the recovery of saleable APT and WO_3 , along with cathodically deposited Co.

For example, Co further treatment by electrorefining may increase its purity. The newly developed methods for recycling WC-Co scraps through electrodisolution routes, and recovering saleable APT and WO_3 very pure, along with cathodically deposited Co, have an advantage compared to conventional processes, such as energy-intensive oxidation for eliminating WC-Co, since they have just a few industrial requirements, limited processing steps, recovered saleable products in simple unit operations, etc. [38].

Conclusions

1. The WC-Co scraps used for the electrodisolution studies contained about 81% W, 10% Co and 5% C, apart from the minor amounts of Fe, Al and Ti. The XRD analysis showed that W was mainly in the WC phase, and Co in the metallic form.
2. The initial polarization studies demonstrated that, without additives in the NH_3 electrolyte, the anodic J was not very high, but it increased significantly with NH_4Cl , $(\text{NH}_4)_2\text{SO}_4$ or $(\text{NH}_4)_2\text{CO}_3$ addition, being the strongest with NH_4Cl increasing amounts.
3. WC-Co scraps dissolution in a NH_3 solution was found to follow the pitting corrosion mechanism, as it was evident from the AFM topographical images.
4. In the electrodisolution studies, it was seen that WC-Co anodic dissolution and J values were enhanced with higher NH_4Cl contents, stronger voltage and increasing NH_3 concentrations. The cathodic deposition achieved its maximum at 10 V, with 5% NH_4Cl in 150 g/L NH_3 .
5. With the abovementioned optimum electrodisolution parameters in NH_3 electrolytes, W recovery was 65.1%, in the 2h experiment. The W in the solution was further treated for producing YTO.

Acknowledgments

The authors are thankful to Dr. R. K. Jana (CSIR-NML), for its help in the PDP experiments. The authors thank the Director (CSIR-NML, Jamshedpur), for his permission to publish this work.

Authors' contributions

Prvan Kumar Katiyar: performed the experiments as per the plan; acquired the necessary data and made the graphical formatting; performed the analysis on literature relevant to the studies; prepared the manuscript and structure in the style of journal article; collected relevant references. **Navneet Singh Randhawa:** conceived building and hypothesis testing; planned the experiments and selected parameters for the studies; analyzed the information collected from the experiments and selected useful data for testing the hypothesis; made the graphical and pictorial representation of the results; interpreted the experimental data for the results and discussion; made the final correction and formatting of the manuscript; acted as corresponding author and as resource person for all the requirements of the present study.

Abbreviations

AFM: atomic force microscopy

APT: ammonium paratungstate

Aqua regia: one part of concentrated HNO₃ mixed with three parts of concentrated HCl

AR: analytical reagents

BCC: body-centered cubic

BSE: backscattered electron image

Co²⁺: cobalt divalent cation

CO₃⁻²: carbonate ions

Co₆W₆C: ternary carbide

DC: direct current

E: potential

EDL: electrical double layer

EDX: energy dispersive X-ray

H₂SO₄: sulfuric acid

H₂WO₄: tungstic acid

H₃PO₄: phosphoric acid

H₈N₂O₄W: ammonium tungstate

HCl: hydrochloric acid

HCP: hexagonal close-packed

HNO₃: nitric acid

ICP-OES: inductively coupled plasma - optical emission spectrometer

J: current density

JCPDS: currently known as ICDD (International Centre for Diffraction Data)

K_α: x-rays produced by transitions from the n=2 to n=1 levels

KCl: potassium chloride

Na₂WO₄: sodium tungstate

NaOH: sodium hydroxide

NH₃: ammonia

NH₄Cl: ammonium chloride

(NH₄)₂CO₃: ammonium carbonate

(NH₄)₂SO₄: ammonium sulfate

NH₄OH: ammonium hydroxide

OCP: open circuit potential

PDP: potentiodynamic polarization

R_a: average surface roughness

RE: reference electrode

SC: saturated calomel

SO₄⁻²: sulfate ions

SR: scan rate

SEM: scanning electron microscopy

ST: stainless steel

W: tungsten

WC-Co: tungsten carbide cobalt-bonded

WE: working electrode

WO₃: tungsten oxide

WO₄²⁻: tungstate ions

XRD: X-ray diffraction

YTO: yellow tungsten oxide

References

1. Katiyar PK, Singh PK, Singh R et al. Modes of failure of cemented tungsten carbide tool bits (WC/Co): A study of wear parts. *Int J Refract Met Hard Mater.* 2016;(54): 27-38. <https://doi.org/10.1016/j.ijrmhm.2015.06.018>
2. Katiyar PK, Randhawa NS. Corrosion behavior of WC-Co tool bits in simulated (concrete, soil, and mine) solutions with and without chloride additions. *Int J Refract Met Hard Mater.* 2019;(85):105062. <https://doi.org/10.1016/j.ijrmhm.2019.105062>
3. Malyshev VV, AI Gab. Resource-saving methods for recycling waste tungsten carbide-cobalt cermets and extraction of tungsten from tungsten concentrates. *Theor Found Chem Eng.* 2007;(41):436-441. <https://doi.org/10.1134/S0040579507040161>
4. Katiyar PK, Randhawa NS, Hait J et al. An overview on different processes for recovery of valuable metals from tungsten carbide scrap. In: *ICNFMM-2014, Nagpur.* 2014:1-11.
5. Furberg A, Arvidsson R, Molander S. Environmental life cycle assessment of cemented carbide (WC-Co) production. *J Clean Prod.* 2019;(209):1126-1138. <https://doi.org/10.1016/j.jclepro.2018.10.272>
6. Lin JC, Lin JY, Jou SP. Selective dissolution of the cobalt binder from scraps of cemented tungsten carbide in acids containing additives. *Hydrometallurgy.* 1996;(43):47-61. [https://doi.org/10.1016/0304-386x\(96\)00023-0](https://doi.org/10.1016/0304-386x(96)00023-0)
7. Joost R, Pirso J, Viljus M et al. Recycling of WC-Co hardmetals by oxidation and carbothermal reduction in combination with reactive sintering. *Est J Eng.* 2012;(12):127-139. <https://doi.org/10.3176/eng.2012.2.03>
8. Lee GG, Ha GH. Effects of mechanical milling on the carbothermal reduction of oxide of WC/Co hardmetal scrap. *Met Mater Int.* 2016;(22):260-266. <https://doi.org/10.1007/s12540-016-5409-y>
9. Mishra D, Sinha S, Sahu KK et al. Recycling of secondary tungsten resources. *Trans Indian Inst Met.* 2017;(70):479-485. <https://doi.org/10.1007/s12666-016-1003-8>
10. Edtmaier C, Schiesser R, Meissl C et al. Selective removal of the cobalt binder in WC/Co based hardmetal scraps by acetic acid leaching. *Hydrometallurgy.* 2005;(76):63-71. <https://doi.org/10.1016/j.hydromet.2004.09.002>

11. Kuntiyi OI, Yavorskyi VT, Ivashkiv VR et al, Four-factor optimization for electrochemical conversion of WC-Ni pseudo alloy in sulfuric acid solutions. *Chem Eng Commun.* 2012;(199):838-848. <https://doi.org/10.1080/00986445.2011.631234>
12. Davydov AD, Shaldaev VS, Malofeeva AN et al. Electrochemical dissolution of tungsten under pulsed conditions. *J Appl Electrochem.* 1997;(27):351-354. <https://doi.org/10.1023/A:1018493016444>
13. Ghandehari MH, Faulkner JK, Schussler M. Selective dissolution of the binder phase alloy (Co-W) from WC-Co cemented carbides in particulate bed electrode systems. *J Electrochem Soc.* 1982;(12):2666-2668. <https://doi.org/10.1149/1.2123643>
14. Vanderpool CD. Electrolytic disintegration of sintered metal carbides. US Patent 4385972. 1983.
15. Niitzel HG. Process for decomposing hard metal scrap. US Patent 4349423. 1982.
16. Vanderpool CD. Recovery of tungsten from heavy metal scrap. US4283258, 981.
17. Katiyar PK, Randhawa NS, Hait J et al. Anodic dissolution behaviour of tungsten carbide scraps in ammoniacal media. *Adv Mater Res.* 2014;(828):11-20. <https://doi.org/10.4028/www.scientific.net/AMR.828.11>
18. Sampath A, Sudarshan TS. Recycling of WC-Co from scrap materials. *Powder Metall.* 2002;(45):21-24. <https://doi.org/10.1179/003258902225001588>
19. Hyo Yang D, Srivastava RR, Kim MS et al. Efficient recycling of WC-Co hardmetal sludge by oxidation followed by alkali and sulfuric acid treatments. *Met Mater Int.* 2016;(22):897-906. <https://doi.org/10.1007/s12540-016-6060-3>
20. Wongsisa S, Srichandr P, Poolthong N. Development of manufacturing technology for direct recycling cemented carbide (WC-Co) tool scraps. *Mater Trans.* 2014;(56):70-77. <https://doi.org/10.2320/matertrans.M2014213>
21. Zaichenko VN, Fomanyuk SS, Krasnov YS et al. Recovery of tungsten and cobalt from secondary raw materials by a combined electrochemical and chemical procedure. *Russ J Appl Chem.* 2010;(83):1660-1662. <https://doi.org/10.1134/S1070427210090284>
22. Makino T, Nagai S, Iskandar F et al. Recovery and Recycling of Tungsten by Alkaline Leaching of Scrap and Charged Amino Group Assisted Precipitation. *ACS Sustain Chem Eng.* 2018;(6):4246-4252. <https://doi.org/10.1021/acssuschemeng.7b04689>
23. Srivastava RR, Lee JC, Bae M et al. Reclamation of tungsten from carbide scraps and spent materials. *J Mater Sci.* 2019;(54):83-107. <https://doi.org/10.1007/s10853-018-2876-1>
24. Abdel-Mawla AO, Taha MA, El-Kady OA et al. Recycling of WC-TiC-TaC-NbC-Co by zinc melt method to manufacture new cutting tools. *Results Phys.* 2019;(13):102092. <https://doi.org/10.1016/j.rinp.2019.02.028>
25. Pee JH, Kim GH, Lee HY et al. Extraction factor of tungsten sources from tungsten scraps by zinc decomposition process. *Arch Metall Mater.* 2015;(60):1311-1314. <https://doi.org/10.1515/amm-2015-0120>
26. Lee J, Lee J, Kim B et al. Leaching behavior of Al, Co and W from the Al-alloying treated WC-Co tool as a new recycling process for WC hard scrap.

- metals. 2016;(6):174. <https://doi.org/10.3390/met6080174>
27. Li M, Xi X, Nie Z et al. Recovery of tungsten from WC-Co hard metal scraps using molten salts electrolysis. *J Mater Res Technol.* 2019;(8):1440-1450. <https://doi.org/10.1016/j.jmrt.2018.10.010>
 28. Lin J-C, Lin J-Y, Lee S-L. Process for recovering tungsten carbide from cemented tungsten carbide scraps by selective electrolysis. US5384016A. 1995.
 29. Lee J, Kim S, Kim B. A new recycling process for tungsten carbide soft scrap that employs a mechanochemical reaction with sodium hydroxide. *Metals.* 2017;(7):230. <https://doi.org/10.3390/met7070230>
 30. Hayashi T, Sato F, Sasaya J et al. Industrialization of tungsten recovering from used cemented carbide tools. *SEI Tech Rev.* 2016:33-38.
 31. Tuvic T, Pašti I, Mentus S. Tungsten electrochemistry in alkaline solutions-anodic dissolution and oxygen reduction reaction. *Russ J Phys Chem A.* 2011;(85):2399-2405. <https://doi.org/10.1134/S0036024411130322>
 32. Malyshev VV, Hab AI. Separation of cobalt and tungsten carbide by anodic dissolution of solid alloys in phosphoric acid. *Mater Sci.* 2004;(40):555-559. <https://doi.org/10.1007/s11003-005-0078-x>
 33. Paul RL, Te Riele WAM, Nicol MJ. A novel process for recycling tungsten carbide scrap. *Int J Miner Process.* 1985;(15):41-56. [https://doi.org/10.1016/0301-7516\(85\)90022-5](https://doi.org/10.1016/0301-7516(85)90022-5)
 34. Vanderpool CD. Electrolytic method for producing ammonium paratungstate from cemented tungsten carbide. US Patent 5021133. 1991.
 35. Xingbo Yang TS, Xiong J. Recycling tungsten carbide. US 2011/0048968 A1. 2011.
 36. Srinivasan GN, Varadharaj A, Abdul Kader JAM. Anodic leaching of tungsten alloy swarf: a statistical approach. *J Appl Electrochem.* 1994;(24):1191-1193. <https://doi.org/10.1007/BF00241321>
 37. Ghandehari MH. Process for recovering metal carbide powder from cemented carbides. US4234333. 1980.
 38. Katiyar PK, Randhawa NS. A comprehensive review on recycling methods for cemented tungsten carbide scraps highlighting the electrochemical techniques. *Int J Refract Met Hard Mater.* 2020;(90):105251. <https://doi.org/10.1016/j.ijrmhm.2020.105251>
 39. Randhawa NS, Katiyar PK. Potentiodynamic polarization behavior and microscopic examination of tungsten carbide hard metal materials in supported ammoniacal medium. *Port Electrochim Acta.* 2020(38):1-27. <https://doi.org/10.4152/pea.202003185>
 40. Hairunnisha S, Sendil GK, Rethinaraj JP et al. Studies on the preparation of pure ammonium para tungstate from tungsten alloy scrap. *Hydrometallurgy.* 2007;(85):67-71. <https://doi.org/10.1016/j.hydromet.2006.08.002>
 41. Ji X, Buzzeo MC, Banks CE et al. Electrochemical response of cobalt (II) in the presence of ammonia. *Electroanalysis.* 2006;(18):44-52. <https://doi.org/10.1002/elan.200503361>

42. Katiyar PK. A comprehensive review on synergy effect between corrosion and wear of cemented tungsten carbide tool bits: A mechanistic approach. *Int J Refract Met Hard Mater.* 2020;(92):1053-15. <https://doi.org/10.1016/j.meegid.2020.104265>
43. Gendel Y, Lahav O. Revealing the mechanism of indirect ammonia electrooxidation. *Electrochim Acta.* 2012;(63):209-219. <https://doi.org/10.1016/j.electacta.2011.12.092>